Extreme ultraviolet and soft x-ray spectral lines in Rb XXIX

Indu Khatri[1,†], Arun Goyal[1], Sunny Aggarwal[1,3], A K Singh[2], and Man Mohan[1]

[1] *Department of Physics and Astrophysics, University of Delhi, Delhi* 110007, *India*
[2] *Department of Physics, D. D. U. College, University of Delhi, Delhi* 110015, *India*
[3] *Department of Physics, Shyamlal College, University of Delhi, Delhi* 110032, *India*

(Received 31 August 2015; revised manuscript received 28 November 2015; published online 25 January 2016)

An extensive theoretical set of atomic data for Rb XXIX in a wide range with *L*-shell electron excitations to the *M*-shell has been reported. We have computed energy levels for the lowest 113 fine structure levels of Rb XXIX. The fully relativistic multiconfigurational Dirac–Fock method (MCDF) within the framework of Dirac–Coulomb Hamiltonian taking quantum electrodynamics (QED) and Breit corrections into account has been adopted for calculations. Radiative data are reported for electric dipole (E1), magnetic dipole (M1), electric quadrupole (E2), and magnetic quadrupole (M2) transitions from the ground level, although calculations have been performed for a much larger number of levels. To assess the accuracy of results, we performed analogous calculations using flexible atomic code (FAC). Comparisons are made with existing available results and a good agreement has been achieved. Most of the wavelengths calculated lie in the soft x-ray (SXR) region. Lifetimes for all 113 levels have also been provided for the first time. Additionally, we have provided the spectra for allowed transitions from $n = 2$ to $n = 3$ within the x-ray region and also compared our SXR photon wavelengths with experimentally recognized wavelengths. We hope that our results will be beneficial in fusion plasma research and astrophysical applications.

Keywords: energy levels, wavelengths, radiative rates, spectral lines

PACS: 32.70.Cs, 32.30.Rj **DOI:** 10.1088/1674-1056/25/3/033201

1. Introduction

As lines from fluorine-like ions have been observed in planetary nebulas,[1] solar flares[2,3] and in the spectra of laboratory plasmas,[4,5] atomic data are needed for diagnostic purposes. The factor which makes F-like configuration absolute for detailed study is the nearly full 2p shell which shows that the spectra are not too complex. The $2s^2 2p^5$–$2s2p^6$ transitions of F-like ions are observed in high-temperature plasmas and can thus be used for plasma diagnostic purposes. Magnetic dipole transitions between fine structure levels separated by spin–orbit interaction such as $2s^2 2p^5\ {}^2P_{3/2}$–$^2P_{1/2}$ transition in fluorine-like ions have important applications in astrophysics[6] and high-temperature plasma diagnostics.[7,8] The transition $2s^2 2p^5\ {}^2P_{3/2}$–$^2P_{1/2}$ is observed in tokamaks and is useful for measuring ion temperatures via Doppler broadening.[9] The emission line ratios involving the $2s^2 2p^5\ {}^2P_{3/2}$, $2s^2 2p^5\ {}^2P_{1/2}$, $2s2p^6\ {}^2S$ levels of fluorine-like ions are useful for plasma diagnostics.[10] Forbidden lines of the fluorine isoelectronic sequence with n_p^k configuration have been identified in tokamak discharges and in the solar corona and flares. As forbidden lines occur at long wavelengths, these are diagnostically important and hence accurate line profiles can be obtained.

The spectroscopy of highly charged ions is of considerable interest in both pure atomic physics and applications such as hot-plasma diagnostics, high temperature astrophysical plasma,[11–13] x-ray laser development and for the study of high-field relativistic and quantum electrodynamic (QED) effects. Transitions in such ions are used to find temperature and density distributions and in calculating stellar envelope opacities.[14] Accurate measurements of energy levels provide tests of modern atomic-structure theory. Accurate atomic data such as transition probabilities, oscillator strengths, and lifetimes of excited levels are requisite in astrophysics, laser spectroscopy, laboratory plasma diagnostic, tokamak devices, and controlled thermonuclear reactions. Accurate atomic data are also needed for reliable interpretation of observed data.[15]

Astrophysical interest in the spectra of multiply charged ions has increased as the maximum number of lines emitted from high Z ions lie within extreme ultraviolet (EUV) 100–1200 Å and soft x-ray (SXR) 1–50 Å regions useful in providing detailed knowledge of coronal atmosphere. Recently, much progress has been made in the study of soft x-ray lasers. The interest in soft x-ray lasers motivates the study of the spectroscopy of highly charged ions.

F-like ions have been studied previously by various authors. Sampson *et al.*[16] calculated transition probabilities between levels of the $2s^2 2p^5$, $2s2p^6$, $2s^2 2p^4 3l$, and $2s2p^5 3l$ configurations using the relativistic distorted wave method. Three lowest energy levels were calculated by Ivanova and Gulov[17] using the relativistic perturbation theory with a model potential. Kim and Huang[18] provided spin–orbit intervals in the ground state $2p^5\ {}^2P_{3/2}$–$^2P_{1/2}$ of F-like ions for $Z \leq 56$. Atomic binding energies for lithium to dubnium isoelectronic series in

†Corresponding author. E-mail: indu.khatri.du@gmail.com

© 2016 Chinese Physical Society and IOP Publishing Ltd

the Dirac–Fock approximation were calculated by Rodrigues *et al.*[19] Gu M F[20] calculated the level energies of $1s^2 2l^q$ ($l \le q \le 8$) states for ions with $Z \le 60$ using a combined configuration interaction and many-body perturbation theory approach. Cheng *et al.*[21] calculated energy levels, oscillator strengths, and transition probabilities for the first row atoms (Li through F) using the multiconfigurational Dirac–Fock method. Transition energies for ions from $Z = 11$ to $Z = 33$ were calculated by Edlén[22] using a semiempirical formula with three adjustable parameters. Some authors[23,24] using the CIV3 code obtained oscillator strengths of transition from the ground state of fluorine-like ions. Nahar[25] obtained atomic data for fluorine-like iron using relativistic Breit–Pauli approximation under the iron project. Fischer and Tachiev[26] obtained energy levels and transition rates for low lying states for ions up to Ti XIV using multiconfigurational Breit–Pauli wavefunctions. Jonauskas *et al.*[27] calculated energy levels and transition probabilities among levels of the ground and first 23 excited configurations of Fe XVIII using multiconfigurational Dirac–Fock method. Energies and E1, M1, E2 transition rates for $2s^2 2p^5$ and $2s2p^6$ configurations states in F-like ions between Si VI and W LXVI were calculated by Jönsson *et al.*[28]

Feldman *et al.*[29] identified transitions of the type 2s–2p in the highly charged fluorine-like Mo, Cd, In, and Sn. Transitions of the type 2s–2p were also identified in F-like As, Se, Br, and Rb by Feldman *et al.*[30] Zigler *et al.*[31] presented wavelengths and identified 11 x-ray lines due to 2p–3d and 2p–3s transitions in Rb XXIX. The *L*-shell soft x-ray emission spectra of Cu, Zn, Ga, As, Br, Rb, and Sr from laser-produced plasma sources for $2p^5$–$2p^4 3s$, 3d fluorine-like transitions were recorded by Hutcheon *et al.*[32] Denis-Petit *et al.* identified x-ray spectra in the Na-like to O-like Rubidium ions in the range 3.8–7.3 Å.[33]

The main focus of our work is to perform fully relativistic calculations in order to obtain transition energies, oscillator strengths, transition rates, and lifetimes for lowest 113 levels of the $2s^2 2p^5$, $2s2p^6$, $2s^2 2p^4 3l$, $2s2p^5 3l$, $2p^6 3l$, $2s^2 2p^4 4l$, $2s2p^5 4l$, $2s^2 2p^4 5l$, and $2s2p^5 5l$ ($l = 0,1,2,3$) configurations of F-like Rb. In the present calculations, we have adopted the relativistic multiconfiguration Dirac–Fock (MCDF) approach. Such calculations including physical effects of the relativistic two-body Breit interaction and the QED corrections provide accurate tools to test the many-body atomic theory and for plasma diagnostics in high temperature plasmas. We have also provided a comparison of our results with the data compiled by NIST.[34,35] We theoretically identified EUV and soft x-ray transitions and plotted the Rb XXIX spectra. This work is an extension of our previous work[36] in which we investigated the spectra of Sr XXX.

2. Theoretical method

To perform large-scale calculations, the fully relativistic MCDF method originally developed by Grant *et al.*[37] and revised by Norrington[38] has been adopted which has successfully been applied earlier by ourselves and others.[39–44] It takes into account all the relativistic effects as well as Breit and QED corrections important for highly ionized atoms.

In the MCDF method, the dominant interactions in an *N*-electron ion or atom are included in the Dirac–Coulomb Hamiltonian

$$\hat{H}^{\mathrm{DC}} = \sum_{i=1}^{N} \hat{H}_i + \sum_{i=1}^{N-1} \sum_{j=i+1}^{N} \frac{1}{|\hat{r}_i - \hat{r}_j|}, \tag{1}$$

where $\hat{H}_i$ denotes the Dirac Hamiltonian of each electron given by

$$\hat{H}_i = c\boldsymbol{\alpha}_i \cdot \boldsymbol{p}_i + \beta mc^2 + V_{\mathrm{nuc}}(r_i). \tag{2}$$

Here, the first two terms denote the kinetic energy of the electron and the Coulomb potential of the nucleus is denoted by the last term, c is the speed of light, α and β represent 4×4 Dirac matrices, and $V_{\mathrm{nuc}}(r_i)$ denotes the electron–nucleus Coulomb interaction.

The relativistic atomic state function of an atom or ion is described by an atomic state function (ASF) constructed approximately by a linear combination of configuration state functions (CSFs) with the same parity P and same angular momentum (J, M)

$$|\psi_\alpha(PJM)\rangle = \sum_{i=1}^{n_c} C_i(\alpha)\,|\gamma_i(PJM)\rangle, \tag{3}$$

where n_c is the number of CSFs considered in the evaluation of ASFs, C_i is the configuration mixing coefficient and denotes the number of electron–electron correlations to be considered, α denotes labeling of the configuration state function such as orbital occupancy, coupling scheme, etc, and $|\gamma_r(PJM)\rangle$ are CSFs specifying a particular state with a given parity and angular momentum (J, M).

The configuration state functions ϕ, are built as linear combinations of Slater determinants which, in the Dirac–Fock model, is a product of one-electron Dirac orbitals

$$\phi(r,\theta,\varphi,\sigma) = \frac{1}{r}\begin{pmatrix} P_{nk}(r) & \chi_{km}(\theta,\varphi,\sigma) \\ -\mathrm{i}Q_{nk}(r) & \chi_{-km}(\theta,\varphi,\sigma) \end{pmatrix}, \tag{4}$$

where $P_{nk}(r)$ and $Q_{nk}(r)$ denote the large and small component one-electron radial wavefunctions required to be orthonormal within each k symmetry. Here, $k = \pm(j+1/2)$ for $l = j \pm 1/2$, k is the Dirac angular quantum number and m is the projection of angular momentum j. In $\chi_{km}(\theta,\varphi,\sigma)$, σ is the electron spin z-projection quantum number, χ_{km} is the spherical harmonics in the *LSJ* coupling scheme defined by

$$\chi_{km}(\theta,\varphi,\sigma) = \sum_{\sigma=\pm\frac{1}{2}} \left\langle lm-\sigma\,\frac{1}{2}\sigma \middle| l\,\frac{1}{2}\,jm \right\rangle Y_l^{m-\sigma}(\theta,\varphi)\,\varphi^\sigma. \tag{5}$$

By the expectation value of Dirac Hamiltonian, the energy of the N-electron system is given as

$$E_{\alpha}^{PJM} = \left\langle \psi_{\alpha}(PJM)|H^{\mathrm{DC}}|\psi_{\alpha}(PJM)\right\rangle, \tag{6}$$

where the Hamiltonian matrix H^{DC} has elements

$$H_{rs}^{\mathrm{DC}} = \left\langle \gamma_r(PJM)|H^{\mathrm{DC}}|\gamma_s(PJM)\right\rangle. \tag{7}$$

For the energy to be stationary with respect to variations in mixing co-efficients $C_i(\alpha)$ and using the orthonormality condition $(C_i(\alpha))^{+}C_j(\alpha) = \delta_{ij}$

$$\left(H^{\mathrm{DC}} - E_{\alpha}^{\mathrm{DC}} I\right) C_{\alpha}^{\mathrm{DC}} = 0, \tag{8}$$

where I is the $n_{\mathrm{c}} \times n_{\mathrm{c}}$ unit matrix. Thus, equation (8) shows that atomic energy level E_{α} can now be taken to be eigenvalues of H^{DC}.

CSFs are obtained from the antisymmetrized products of a common set of orthonormal orbitals which are optimized on the basis of Dirac–Coulomb Hamiltonian. By solving the MCDF equations, the radial functions are determined which depend upon varying the orbital radial functions to obtain an extremum of the energy functional. The wavefunction is expanded to thousands of CSFs and thus enables us to obtain a suitable description of level structure and transition properties for multiple and highly charged ions. Relativistic configuration interaction calculations are then carried out to evaluate CSF expansion coefficients by diagonalizing the Hamiltonian matrix. After obtaining self consistency, the contributions from the Breit interaction, vacuum polarization, self-energy and finite nuclear mass corrections are added as a first-order perturbation correction.

To calculate the radial wavefunctions, we have adopted the extended average-level (EAL) mode for self-consistent calculations in which a weighted trace of the Hamiltonian matrix is minimized. It can assign a configuration of a given weight automatically.

To assess the accuracy of our results from MCDF, we employ another fully relativistic code, the flexible atomic code (FAC)[45] based on Dirac equation. The atomic structure calculations are based on the relativistic configuration-interaction (CI) method. In FAC, the basis state functions are built by radial spinors obtained from a modified Dirac–Fock–Slater central field potential. The orbitals are optimized self-consistently where the average energy of a fictitious mean configuration with fractional orbital occupation numbers is minimized. This mean configuration stands for the average electron cloud of the configurations maintained in the configuration–interaction (CI) expansion. Using the Dirac–Coulomb Hamiltonian, relativistic effects are fully considered. Generally, there is no major discrepancy in the determination of energy levels and radiative data from FAC and MCDF. MCDF provides more options in terms of optimization schemes. The results from FAC will be helpful in assessing the accuracy of energy levels, radiative rates, and oscillator strengths.

3. Results and discussion

3.1. Energy levels

As velocity of electrons in the highly ionized atoms is fast and the nuclear potential energy is very strong, the relativistic effects must be taken into account. Therefore, in this work, calculations have been performed using fully relativistic MCDF approach. As an elaborate CI is needed to achieve a better accuracy, therefore we have included CI among $2s^22p^5$, $2s2p^6$, $2s^22p^43l$, $2s2p^53l$, $2p^63l$, $2s^22p^44l$, $2s2p^54l$, $2s^22p^45l$, and $2s2p^55l$ configurations, where ($l = \mathrm{s,p,d,f}$). We included correlation effects in the excitation up to the 5f orbital. In the last column of Table 1, we have also listed the mixing coefficients for these 113 levels. We find that some of the levels such as $2s^22p^5\ {}^2P^o_{3/2}$, $2s^22p^5\ {}^2P^o_{1/2}$, and $2s2p^6\ {}^2S_{1/2}$ are almost pure. Due to clear dominance, some of the levels can be easily identified such as $2s^22p^4\ (^3_2P)\ 3s\ {}^4P_{3/2}$. But some levels are strongly mixed, for example $2s^22p^4\ (^1S)\ 3p\ {}^2P^o$ is strongly mixed with $2s^22p^4\ (^3_2P)\ 3p\ {}^4D^o$, and $2s2p^5\ (^2_1P)\ 3s\ {}^4P^o$ with their compositions being 34%, 31%, and 28%. Therefore, identification of a particular level becomes difficult. Further, we notice that the levels $2s^22p^4\ (^1S)\ 3s\ {}^2S_{1/2}$ and $2s^22p^4\ (^3_2P)\ 3s\ {}^4P_{1/2}$ can be interchanged due to strong mixing between them. As *LSJ* coupling is not accurate for highly mixed levels, the corresponding *jj* designations for the levels have also been provided under the column "*JJ* coupling". The first number under this column represents the leading percentage of the level and p^-, p, d^-, d denote $p_{1/2}, p_{3/2}, d_{3/2}$ and $d_{5/2}$ respectively.

Table 1. Level No., wave-function compositions and lifetimes of first 113 fine structure levels of Rb XXIX using MCDF.

S. No.	Configuration	$2J$	Lifetime	Composition	
				JJ coupling	*LSJ* coupling
1	$2s^22p^5\ {}^2P^o$	3	–	**100** $2s^22p^{-2}2p^3$	100
2	$2s^22p^5\ {}^2P^o$	1	4.40×10^{-7}	**100** $2s^22p^{-1}2p^4$	100
3	$2s2p^6\ {}^2S$	1	3.29×10^{-12}	**100** $2s^22p^{-2}\ 2p^4$	100
4	$2s^22p^4\ (^3_2P)\ 3s\ {}^4P$	5	9.09×10^{-13}	**98** $2s^22p^{-2}2p^2\ (2)3s$	79+21(7)
5	$2s^22p^4\ (^3_2P)\ 3s\ {}^2P$	3	1.01×10^{-13}	**98** $2s^22p^{-2}2p^2\ (2)3s$	60+24(42)

Table 1. (*Continued*).

S. No.	Configuration	2*J*	Lifetime	Composition	
				JJ coupling	*LSJ* coupling
6	$2s^22p^4$ (^{1}S) 3s ^{2}S	1	2.33×10^{-13}	**96** $2s^22p^{-2}2p^2(0)$ 3s	50+37(35)
7	$2s^22p^4$ ($^3_2$P) 3p ^{4}P^o	3	5.62×10^{-11}	**97** $2s^22p^{-2}2p^2(2)$ $3p^{-1}$	41+17(17)
8	$2s^22p^4$ ($^3_2$P) 3p ^{4}D^o	5	5.08×10^{-11}	**95** $2s^22p^{-2}2p^2(2)$ $3p^{-1}$	32+23(27)+23(14)
9	$2s^22p^4$ ($^3_2$P) 3s ^{4}P	3	3.79×10^{-13}	**99** $2s^22p^{-1}2p^3(1)$ 3s	82+16(48)
10	$2s^22p^4$ ($^3_2$P) 3s ^{2}P	1	9.80×10^{-14}	**99** $2s^22p^{-1}2p^3(1)$ 3s	68+31(6)
11	$2s^22p^4$ ($^3_2$P) 3p ^{2}P^o	1	4.32×10^{-11}	**69** $2s^22p^{-2}2p^2(2)$ 3p	28+22(38)+19(24)
12	$2s^22p^4$ ($^3_2$P) 3p ^{2}D^o	5	4.24×10^{-11}	**94** $2s^22p^{-2}2p^2(2)$ 3p	41+37(14)
13	$2s^22p^4$ ($^3_2$P) 3p ^{4}D^o	7	4.83×10^{-11}	**98** $2s^22p^{-2}2p^2(2)$ 3p	77+22(59)
14	$2s^22p^4$ (^{1}S) 3p ^{2}P^o	1	1.61×10^{-11}	**67** $2s^22p^{-2}2p^2(0)$ $3p^{-1}$	34+31(18)+28(61)
15	$2s^22p^4$ ($^1_2$D) 3s ^{2}D	5	1.96×10^{-13}	**98** $2s^22p^{-1}2p^3(2)$ 3s	78+21(4)
16	$2s^22p^4$ ($^1_2$D) 3s ^{2}D	3	1.32×10^{-13}	**98** $2s^22p^{-1}2p^3(2)$ 3s	74+24(48)
17	$2s^22p^4$ ($^3_2$P) 3p ^{4}S^o	3	1.25×10^{-11}	**82** $2s^22p^{-2}2p^2(2)$ 3p	33+21(39)+20(13)
18	$2s^22p^4$ ($^3_2$P) 3p ^{4}D^o	3	3.32×10^{-11}	**80** $2s^22p^{-2}2p^2(0)$ 3p	41+33(31)
19	$2s^22p^4$ ($^3_2$P) 3p ^{4}P^o	1	1.39×10^{-10}	**95** $2s^22p^{-1}2p^3(1)$ $3p^{-1}$	60+19(18)+17(61)
20	$2s^22p^4$ ($^3_2$P) 3p ^{2}P^o	3	4.33×10^{-11}	**71** $2s^22p^{-1}2p^3(1)$ $3p^{-1}$	40+23(39)
21	$2s^22p^4$ ($^1_2$D) 3p ^{2}F^o	5	5.65×10^{-11}	**97** $2s^22p^{-1}2p^3(2)$ $3p^{-1}$	61+16(22)
22	$2s^22p^4$ ($^3_2$P) 3p ^{4}P^o	5	4.93×10^{-11}	**97** $2s^22p^{-1}2p^3(1)$ 3p	60+23(27)
23	$2s^22p^4$ ($^3_2$P) 3d ^{4}D	3	3.58×10^{-12}	**95** $2s^22p^{-2}2p^2(2)$ $3d^{-1}$	42+21(12)
24	$2s^22p^4$ ($^3_2$P) 3d ^{4}D	5	5.13×10^{-11}	**83** $2s^22p^{-2}2p^2(2)$ $3d^{-1}$	55
25	$2s^22p^4$ ($^3_2$P) 3p ^{2}S^o	1	3.99×10^{-11}	**74** $2s^22p^{-1}2p^3(1)$ 3p	32+19(32)+19(18)
26	$2s^22p^4$ ($^3_2$P) 3p ^{2}D^o	3	2.93×10^{-11}	**95** $2s^22p^{-1}2p^3(1)$ 3p	51+24(17)+21(55)
27	$2s^22p^4$ ($^3_2$P) 3d ^{4}P	1	6.91×10^{-13}	**79** $2s^22p^{-2}2p^2(2)$ $3d^{-1}$	31+24(21)+23(9)
28	$2s^22p^4$ ($^3_2$P) 3d ^{4}D	7	5.95×10^{-11}	**56** $2s^22p^{-2}2p^2(2)$ 3d	50+30(60)
29	$2s^22p^4$ ($^3_2$P) 3d ^{4}F	9	7.04×10^{-11}	**99** $2s^22p^{-2}2p^2(2)$ 3d	77+23(40)
30	$2s^22p^4$ ($^3_2$P) 3d ^{2}F	7	5.26×10^{-11}	**58** $2s^22p^{-2}2p^2(2)$ $3d^{-1}$	59+22(49)
31	$2s^22p^4$ ($^1_2$D) 3p ^{2}P^o	3	6.65×10^{-12}	**54** $2s^22p^{-1}2p^3(2)$ 3p	65+18(17)
32	$2s^22p^4$ ($^3_2$P) 3d ^{2}P	1	3.53×10^{-14}	**77** $2s^22p^{-2}2p^2(2)$ 3d	40+30(46)+22(34)
33	$2s^22p^4$ ($^1_2$D) 3p ^{2}F^o	7	3.54×10^{-11}	**98** $2s^22p^{-1}2p^3(2)$ 3p	77+22(19)
34	$2s^22p^4$ ($^1_2$D) 3p ^{2}D^o	3	1.62×10^{-11}	**50** $2s^22p^{-1}2p^3(2)$ $3p^{-1}$	59+37(39)
35	$2s^22p^4$ ($^3_2$P) 3s ^{4}P	1	8.36×10^{-14}	**94** $2s^22p^4(0)$ 3s	47+30(6)+18(10)
36	$2s^22p^4$ ($^3_2$P) 3d ^{4}P	3	2.98×10^{-14}	**70** $2s^22p^{-2}2p^2(2)$ 3d	33+27(16)
37	$2s^22p^4$ ($^1_2$D) 3p ^{2}D^o	5	2.90×10^{-11}	**96** $2s^22p^{-1}2p^3(2)$ 3p	65
38	$2s^22p^4$ ($^3_2$P) 3d ^{4}P	5	2.08×10^{-14}	**78** $2s^22p^{-2}2p^2(2)$ 3d	28+23(45)+22(43)
39	$2s^22p^4$ (^{1}S) 3d ^{2}D	3	3.40×10^{-14}	**68** $2s^22p^{-2}2p^2(0)$ $3d^{-1}$	35+33(36)+21(53)
40	$2s^22p^4$ ($^3_2$P) 3d ^{4}F	5	2.72×10^{-14}	**84** $2s^22p^{-2}2p^2(0)$ 3d	43+26(56)
41	$2s^22p^4$ ($^1_2$D) 3p ^{2}P^o	1	2.86×10^{-12}	**73** $2s^22p^{-1}2p^3(2)$ 3p	52+23(32)
42	$2s^22p^4$ ($^3_2$P) 3d ^{4}D	1	2.09×10^{-12}	**92** $2s^22p^{-1}2p^3(1)$ $3d^{-1}$	75
43	$2s^22p^4$ ($^3_2$P) 3d ^{4}F	3	3.72×10^{-13}	**70** $2s^22p^{-1}2p^3(1)$ $3d^{-1}$	39+19(36)
44	$2s^22p^4$ ($^3_2$P) 3d ^{4}F	7	7.14×10^{-11}	**97** $2s^22p^{-1}2p^3(1)$ 3d	49+33(5)
45	$2s^22p^4$ ($^3_2$P) 3d ^{2}D	5	4.09×10^{-14}	**64** $2s^22p^{-1}2p^3(1)$ $3d^{-1}$	48+24(28)
46	$2s^22p^4$ ($^3_2$P) 3d ^{2}F	5	1.28×10^{-13}	**77** $2s^22p^{-1}2p^3(1)$ 3d	58+27(45)
47	$2s^22p^4$ ($^3_2$P) 3d ^{2}P	3	1.34×10^{-13}	**58** $2s^22p^{-1}2p^3(1)$ 3d	38+16(41)
48	$2s^22p^4$ ($^3_2$P) 3p ^{4}D^o	1	3.94×10^{-11}	**89** $2s^22p^4(0)3p^{-1}$	42+27(32)+18(18)
49	$2s^22p^4$ ($^1_2$D) 3d ^{2}G	7	4.69×10^{-11}	**99** $2s^22p^{-1}2p^3(2)$ $3d^{-1}$	69
50	$2s^22p^4$ ($^1_2$D) 3d ^{2}G	9	7.34×10^{-11}	**99** $2s^22p^{-1}2p^3(2)$ 3d	77+23(44)
51	$2s^22p^4$ ($^1_2$D) 3d ^{2}S	1	1.18×10^{-14}	**78** $2s^22p^{-1}2p^3(2)$ $3d^{-1}$	65+22(29)
52	$2s^22p^4$ (^{1}S) 3p ^{2}P	3	1.05×10^{-11}	**95** $2s^22p^4(0)$ $3p^1$	48
53	$2s^22p^4$ ($^1_2$D) 3d ^{2}D	5	2.82×10^{-13}	**94** $2s^22p^{-1}2p^3(2)$ 3d	59+21(20)
54	$2s^22p^4$ ($^1_2$D) 3d ^{2}P	3	1.03×10^{-14}	**47** $2s^22p^{-1}2p^3(2)$ $3d^{-1}$	57
55	$2s^22p^4$ ($^1_2$D) 3d ^{2}F	7	6.02×10^{-11}	**95** $2s^22p^{-1}2p^3(2)$ 3d	73
56	$2s^22p^4$ ($^1_2$D) 3d ^{2}F	5	1.22×10^{-14}	**84** $2s^22p^{-1}2p^3(2)$ $3d^{-1}$	47+23(28)+18(58)
57	$2s^22p^4$ ($^1_2$D) 3d ^{2}D	3	8.93×10^{-15}	**43** $2s^22p^{-1}2p^3(2)$ 3d	57+30(16)
58	$2s2p^5$ ($^2_1$P) 3s ^{4}P^o	5	6.03×10^{-12}	**99** $2s2p^{-2}2p^3(2)$ 3s	99
59	$2s^22p^4$ ($^1_2$D) 3d ^{2}P	1	6.67×10^{-15}	**79** $2s^22p^{-1}2p^3(2)$ 3d	52+35(46)
60	$2s2p^5$ ($^2_1$P) 3s ^{2}P^o	3	1.85×10^{-13}	**92** $2s2p^{-2}2p^3(2)$ 3s	61+36(66)
61	$2s2p^5$ ($^2_1$P) 3s ^{4}P^o	3	1.19×10^{-12}	**75** $2s2p^{-2}2p^3(1)$ 3s	43+33(75)+22(26)
62	$2s2p^5$ ($^2_1$P) 3s ^{2}P^o	1	1.41×10^{-13}	**82** $2s2p^{-2}2p^3(1)$ 3s	37+40(71)+27(68)
63	$2s2p^5$ ($^2_1$P) 3p ^{4}S	3	8.43×10^{-13}	**93** $2s2p^{-2}2p^3(2)$ $3p^{-1}$	49+38(69)
64	$2s^22p^4$ (^{1}S) 3d ^{2}D	5	5.41×10^{-12}	**93** $2s^22p^4(0)$ 3d	47

Table 1. (*Continued*).

S. No.	Configuration	2*J*	Lifetime	Composition	
				JJ coupling	*LSJ* coupling
65	$2s2p^5$ ($^2_1$P) 3p ^{2}D	5	1.50×10^{-13}	**95** $2s2p^{-2}2p^3(2)\ 3p^{-1}$	45+35(81)+16(70)
66	$2s^22p^4$ ($^3_2$P) 3d ^{2}D	3	1.20×10^{-14}	**93** $2s^22p^4(0)3d^{-1}$	46+18(36)+16(16)
67	$2s2p^5$ ($^2_1$P) 3p ^{4}D	7	6.69×10^{-12}	**99** $2s2p^{-2}2p^3(2)\ 3p$	99
68	$2s2p^5$ ($^2_1$P) 3s ^{4}P^o	1	2.21×10^{-13}	**96** $2s2p^{-1}2p^4(0)\ 3s$	61+35(30)
69	$2s2p^5$ ($^2_1$P) 3p ^{2}P	3	1.02×10^{-13}	**82** $2s2p^{-2}2p^3(2)\ 3p$	38+24(76)+21(83)
70	$2s2p^5$ ($^2_1$P) 3p ^{4}P	5	1.06×10^{-13}	**99** $2s2p^{-2}2p^3(2)3p$	53+44(81)
71	$2s2p^5$ ($^2_1$P) 3p ^{4}P	1	8.00×10^{-13}	**59** $2s2p^{-2}2p^3(1)\ 3p^{-1}$	45+28(106)
72	$2s2p^5$ ($^2_1$P) 3p ^{4}D	3	7.74×10^{-14}	**73** $2s2p^{-2}2p^3(1)\ 3p^{-1}$	43+31(83)+19(80)
73	$2s2p^5$ ($^2_1$P) 3p ^{2}S	1	3.45×10^{-14}	**57** $2s2p^{-2}2p^3(2)\ 3p$	40+38(86)+18(74)
74	$2s2p^5$ ($^2_1$P) 3p ^{4}D	5	1.02×10^{-13}	**82** $2s2p^{-2}2p^3(1)\ 3p$	38+25(73)+22(70)
75	$2s2p^5$ ($^2_1$P) 3p ^{2}D	3	1.50×10^{-13}	**78** $2s2p^{-2}2p^3(1)\ 3p$	37+26(69)+17(82)
76	$2s2p^5$ ($^2_1$P) 3s ^{2}P^o	3	1.54×10^{-13}	**80** $2s2p^{-1}2p^4(1)\ 3s$	76+19(66)
77	$2s2p^5$ ($^2_1$P) 3s ^{2}P^o	1	2.55×10^{-12}	**84** $2s2p^{-1}2p^4(1)\ 3s$	69+26(30)
78	$2s2p^5$ ($^2_1$P) 3p ^{4}D	1	5.21×10^{-13}	**52** $2s2p^{-2}2p^3(1)\ 3p$	39+30(106)
79	$2s2p^5$ ($^2_1$P) 3p ^{2}P	1	7.65×10^{-14}	**76** $2s2p^{-1}2p^4(0)\ 3p^{-1}$	35+34(86)+21(92)
80	$2s2p^5$ ($^2_1$P) 3d ^{4}P^o	1	5.48×10^{-12}	**94** $2s2p^{-2}2p^3(2)\ 3d^{-1}$	94
81	$2s2p^5$ ($^2_1$P) 3d ^{4}P^o	3	5.04×10^{-12}	**79** $2s2p^{-2}2p^3(2)\ 3d^{-1}$	75+24(85)
82	$2s2p^5$ ($^2_1$P) 3d ^{4}F^o	9	8.22×10^{-12}	**100** $2s2p^{-2}2p^3(2)\ 3d$	100
83	$2s2p^5$ ($^2_1$P) 3d ^{4}D^o	5	6.65×10^{-12}	**71** $2s2p^{-2}2p^3(2)\ 3d^{-1}$	50+33(107)+16(99)
84	$2s2p^5$ ($^2_1$P) 3d ^{4}F^o	7	6.82×10^{-12}	**82** $2s2p^{-2}2p^3(2)\ 3d^{-1}$	63+22(101)
85	$2s2p^5$ ($^2_1$P) 3p ^{4}P	3	1.48×10^{-13}	**99** $2s2p^{-1}2p^4(0)\ 3p$	30+28(64)+27(83)
86	$2s2p^5$ ($^2_1$P) 3d ^{4}P^o	5	5.12×10^{-12}	**63** $2s2p^{-2}2p^3(2)\ 3d$	41+21(107)+21(99)
87	$2s2p^5$ ($^2_1$P) 3d ^{2}F^o	7	5.05×10^{-12}	**84** $2s2p^{-2}2p^3(2)\ 3d$	58+41(101)
88	$2s2p^5$ ($^2_1$P) 3d ^{2}D^o	3	6.37×10^{-14}	**62** $2s2p^{-2}2p^3(2)\ 3d$	39+22(79)
89	$2s2p^5$ ($^2_1$P) 3p ^{2}D	3	9.23×10^{-14}	**81** $2s2p^{-1}2p^4(1)\ 3p^{-1}$	62
90	$2s2p^5$ ($^2_1$P) 3d ^{4}D^o	1	1.33×10^{-14}	**77** $2s2p^{-2}2p^3(2)\ 3d$	51+45(97)
91	$2s2p^5$ ($^2_1$P) 3d ^{2}P^o	1	7.26×10^{-14}	**77** $2s2p^{-2}2p^3(1)\ 3d^{-1}$	41+31(103)+26(104)
92	$2s2p^5$ ($^2_1$P) 3d ^{2}D^o	5	3.35×10^{-12}	**78** $2s2p^{-2}2p^3(1)\ 3d^{-1}$	37+27(94)+24(91)
93	$2s2p^5$ ($^2_1$P) 3d ^{4}D^o	3	2.91×10^{-13}	**51** $2s2p^{-2}2p^3(1)\ 3d^{-1}$	22+20(85)+17(90)
94	$2s2p^5$ ($^2_1$P) 3p ^{2}P	1	3.24×10^{-12}	**80** $2s2p^{-2}2p^3(1)\ 3d$	65+18(92)
95	$2s2p^5$ ($^2_1$P) 3d ^{4}D^o	7	5.54×10^{-14}	**50** $2s2p^{-1}2p^4(1)\ 3p^{-1}$	27+26(89)+24(105)
96	$2s2p^5$ ($^2_1$P) 3d ^{2}F^o	5	3.62×10^{-12}	**74** $2s2p^{-2}2p^3(1)\ 3d$	36+22(99)+19(72)
97	$2s2p^5$ ($^2_1$P) 3p ^{2}D	5	4.25×10^{-13}	**82** $2s2p^{-1}2p^4(1)\ 3p$	74
98	$2s2p^5$ ($^2_1$P) 3p ^{2}P	3	9.41×10^{-14}	**80** $2s2p^{-1}2p^4(1)\ 3p$	65
99	$2s2p^5$ ($^2_1$P) 3p ^{2}S	1	5.51×10^{-13}	**42** $2s2p^{-1}2p^4(1)\ 3p$	70
100	$2s2p^5$ ($^2_1$P) 3d ^{2}P^o	3	1.55×10^{-14}	**51** $2s2p^{-2}2p^3(1)\ 3d$	25+24(79)+23(85)
101	$2s2p^5$ ($^2_1$P) 3d ^{4}F^o	5	4.41×10^{-12}	**98** $2s2p^{-1}2p^4(0)\ 3d$	29+25(84)+19(107)
102	$2s2p^5$ ($^2_1$P) 3d ^{4}F^o	3	2.45×10^{-14}	**86** $2s2p^{-1}2p^4(0)\ 3d^{-1}$	36+27(98)+21(91)
103	$2s2p^5$ ($^2_1$P) 3d ^{2}F^o	5	2.21×10^{-12}	**78** $2s2p^{-1}2p^4(1)\ 3d^{-1}$	57+18(72)
104	$2s2p^5$ ($^2_1$P) 3d ^{2}F^o	7	2.40×10^{-12}	**82** $2s2p^{-1}2p^4(1)\ 3d$	75
105	$2s2p^5$ ($^2_1$P) 3d ^{2}P^o	3	2.14×10^{-14}	**71** $2s2p^{-1}2p^4(1)\ 3d$	74
106	$2s2p^5$ ($^2_1$P) 3d ^{2}P^o	1	8.38×10^{-15}	**83** $2s2p^{-1}2p^4(1)\ 3d^{-1}$	67+17(104)
107	$2s2p^5$ ($^2_1$P) 3d ^{2}D^o	5	2.18×10^{-12}	**76** $2s2p^{-1}2p^4(1)\ 3d$	61
108	$2s2p^5$ ($^2_1$P) 3d ^{2}D^o	3	2.85×10^{-14}	**72** $2s2p^{-1}2p^4(1)\ 3d^{-1}$	67+20(98)
109	$2p^6$ 3s ^{2}S	1	1.31×10^{-12}	**96** $2p^{-2}2p^4(0)\ 3s$	96
110	$2p^6$ 3p ^{2}P^o	1	8.04×10^{-14}	**97** $2p^{-2}2p^4(0)\ 3p^{-1}$	97
111	$2p^6$ 3p ^{2}P^o	3	7.61×10^{-14}	**97** $2p^{-2}2p^4(0)\ 3p$	97
112	$2p^6$ 3d ^{2}D	3	1.18×10^{-12}	**98** $2p^{-2}2p^4(0)\ 3d^{-1}$	98
113	$2p^6$ 3d ^{2}D	5	1.38×10^{-12}	**98** $2p^{-2}2p^4(0)\ 3d$	98

In Table 2, we list our calculated energy levels of Rb XXIX, obtained from the MCDF wavefunctions with and without the inclusion of Breit and QED effects. We performed relativistic calculations and included 113 fine structure levels belonging to $2s^22p^5$, $2s2p^6$, $2s^22p^43s$, $2s^22p^43p$, $2s^22p^43d$, $2s2p^53s$, $2s2p^53p$, $2s2p^53d$, $2p^63s$, $2p^63p$, and $2p^63d$ configurations. Our Breit and QED corrected energies are lower than the corresponding Coulomb energies by up to ~ 0.33 Ryd. for a majority of levels. Our level energies without Breit and QED effects differ from the NIST values by (~ 0.57 Ryd). Energies differ from NIST values by a maximum of (~ 0.43 Ryd.) with the inclusion of Breit and QED effects, therefore we can

deduce that higher relativistic effects for heavy ions are very important. Breit contribution to our results is up to 0.0216 Ryd. whereas QED contribution is up to 0.0258 Ryd. Further, it is seen that QED corrections are greater in magnitude for levels where single excitation from 2p to 3s occurs than excitations from 2p to 3p or 3d orbitals such as for $2s^22p^4$ ($^3_2$P) 3s $^4P_{3/2}$. The energy levels are arranged in ascending order. The present calculated values of the energy levels are compared with those calculated by Jönsson *et al.*[28] and with the compiled data from NIST.[34,35] To show the genuineness and credibility of our results, we performed another fully relativistic configuration interaction calculation important for highly ionized plasma using FAC. It is also a fully relativistic code based on jj coupling and results calculated are comparable to MCDF. In Table 2, we list the corresponding energies obtained from the FAC. All combinations of the $2s^22p^5$, $2s2p^6$, $2s^22p^43l$ ($l = 0,1,2$), $2s^22p^44l$ ($l = 0,1,2,3$), $2s^22p^45l$ ($l = 0,1,2,3,4$), $2s2p^53l$ ($l = 0,1,2$), $2s2p^54l$ ($l = 0,1,2,3$), $2s2p^55l$ ($l = 0,1,2,3,4$), $2p^63l$ ($l = 0,1,2$), $2p^64l$ ($l = 0,1,2,3$), $2p^65l$ ($l =$ and 0, 1, 2, 3, 4) configurations have been included in the calculations.

Table 2. Dirac–Coulomb (DC), Breit and quantum electrodynamics (QED) contributions to the MCDF energy (in Ryd) for the lowest 113 levels for Rb XXIX. The sum total is compared with FAC and other available results. All energies are relative to the ground state.

S. No.	Configuration	2J	MCDF				Other results	FAC
			DC	Breit	QED	Total		
1	$2s^22p^5\ ^2P^o$	3	0.0000	–	–	0.0000	0.0000	0.0000
2	$2s^22p^5\ ^2P^o$	1	4.6682	–0.0896	0.0086	4.5872	4.5962[b] 4.5967[a]	4.5882
3	$2s2p^6\ ^2S$	1	18.5520	0.0216	–0.0952	18.4784	18.3250[b] 18.3235[a]	18.4741
4	$2s^22p^4$ ($^3_2$P) 3s ^4P	5	134.7960	–0.1530	0.0175	134.6605		134.6738
5	$2s^22p^4$ ($^3_2$P) 3s ^2P	3	135.1636	–0.1480	0.0175	135.0331	135.186[b]	135.0642
6	$2s^22p^4$ (^{1}S) 3s ^2S	1	136.3911	–0.0947	0.0169	136.3133		136.3135
7	$2s^22p^4$ ($^3_2$P) 3p $^4P^o$	3	138.4960	–0.1100	–0.0071	138.3789		138.3901
8	$2s^22p^4$ ($^3_2$P) 3p $^4D^o$	5	138.6726	–0.1300	–0.0069	138.5355		138.5527
9	$2s^22p^4$ ($^3_2$P) 3s ^4P	3	139.2488	–0.2070	0.0258	139.0671		139.0833
10	$2s^22p^4$ ($^3_2$P) 3s ^2P	1	139.5481	–0.2080	0.0258	139.3662		139.3979
11	$2s^22p^4$ ($^3_2$P) 3p $^2P^o$	1	139.5987	–0.1220	–0.0062	139.4703		139.4711
12	$2s^22p^4$ ($^3_2$P) 3p $^2D^o$	5	139.7561	–0.1530	–0.0051	139.5985		139.6122
13	$2s^22p^4$ ($^3_2$P) 3p $^4D^o$	7	139.8256	–0.1560	–0.0049	139.6644		139.6774
14	$2s^22p^4$ (^{1}S) 3p $^2P^o$	1	140.2988	–0.0869	–0.0066	140.2053		140.0783
15	$2s^22p^4$ ($^1_2$D) 3s ^2D	5	140.3150	–0.2670	0.0257	140.0737	140.153[b]	140.2109
16	$2s^22p^4$ ($^1_2$D) 3s ^2D	3	140.4371	–0.2610	0.0258	140.2015		140.2139
17	$2s^22p^4$ ($^3_2$P) 3p $^4S^o$	3	141.0432	–0.1300	–0.0046	140.9088		140.9394
18	$2s^22p^4$ ($^3_2$P) 3p $^4D^o$	3	141.5432	–0.1040	–0.0050	141.4346		141.4392
19	$2s^22p^4$ ($^3_2$P) 3p $^4P^o$	1	142.8596	–0.1790	0.0014	142.6824		142.6918
20	$2s^22p^4$ ($^3_2$P) 3p $^2P^o$	3	143.2514	–0.1980	0.0013	143.0546		143.0641
21	$2s^22p^4$ ($^1_2$D) 3p $^2F^o$	5	144.0542	–0.2460	0.0014	143.8091		143.8121
22	$2s^22p^4$ ($^3_2$P) 3p $^4P^o$	5	144.1538	–0.2070	0.0031	143.9498		143.9610
23	$2s^22p^4$ ($^3_2$P) 3d ^4D	3	144.3379	–0.1340	–0.0064	144.1977		144.1779
24	$2s^22p^4$ ($^3_2$P) 3d ^4D	5	144.3496	–0.1600	–0.0063	144.1832		144.1898
25	$2s^22p^4$ ($^3_2$P) 3p $^2S^o$	1	144.4061	–0.2150	0.0032	144.1938		144.2032
26	$2s^22p^4$ ($^3_2$P) 3p $^2D^o$	3	144.4397	–0.2040	0.0033	144.2387		144.2595
27	$2s^22p^4$ ($^3_2$P) 3d ^4P	1	144.4851	–0.1430	–0.0064	144.3354		144.3053
28	$2s^22p^4$ ($^3_2$P) 3d ^4D	7	144.4920	–0.1790	–0.0062	144.3072		144.3283
29	$2s^22p^4$ ($^3_2$P) 3d ^4F	9	144.7683	–0.1860	–0.0062	144.5758		144.5752
30	$2s^22p^4$ ($^3_2$P) 3d ^2F	7	144.7882	–0.1760	–0.0062	144.6061		144.6014
31	$2s^22p^4$ ($^1_2$D) 3p $^2P^o$	3	145.1666	–0.2250	0.0015	144.9435		144.9507
32	$2s^22p^4$ ($^3_2$P) 3d ^2P	1	145.2153	–0.1750	–0.0054	145.0352		144.9568
33	$2s^22p^4$ ($^1_2$D) 3p $^2F^o$	7	145.2212	–0.2740	0.0035	144.9505		145.0401
34	$2s^22p^4$ ($^1_2$D) 3p $^2D^o$	3	145.3542	–0.2210	0.0021	145.1353		145.1243
35	$2s^22p^4$ ($^3_2$P) 3s ^4P	1	145.3666	–0.2740	0.0312	145.1234		145.1658
36	$2s^22p^4$ ($^3_2$P) 3d ^4P	3	145.5207	–0.1470	–0.0065	145.3673	145.775[b]	145.3058
37	$2s^22p^4$ ($^1_2$D) 3p $^2D^o$	5	145.5487	–0.2550	0.0032	145.2974		145.3617
38	$2s^22p^4$ ($^3_2$P) 3d ^4P	5	145.8335	–0.1700	–0.0061	145.6577		145.6576
39	$2s^22p^4$ (^{1}S) 3d ^2D	3	146.2818	–0.1240	–0.0064	146.1509		146.1324
40	$2s^22p^4$ ($^3_2$P) 3d ^4F	5	146.5799	–0.1310	–0.0065	146.4421	146.249[b]	146.4258

Table 2. (*Continued*).

S. No.	Configuration	2*J*	MCDF				Other results	FAC
			DC	Breit	QED	Total		
41	$2s^22p^4$ ($^1_2$D) 3p ^{2}P^o	1	146.7752	–0.2280	0.0032	146.5503		146.5881
42	$2s^22p^4$ ($^3_2$P) 3d ^{4}D	1	148.5786	–0.2040	0.0019	148.3762		148.3757
43	$2s^22p^4$ ($^3_2$P) 3d ^{4}F	3	148.9348	–0.2190	0.0020	148.7177		148.7156
44	$2s^22p^4$ ($^3_2$P) 3d ^{4}F	7	149.0749	–0.2380	0.0019	148.8389		148.8353
45	$2s^22p^4$ ($^3_2$P) 3d ^{2}D	5	149.3330	–0.2340	0.0019	149.1006	149.220[b]	149.0987
46	$2s^22p^4$ ($^3_2$P) 3d ^{2}F	5	149.4764	–0.2290	0.0020	149.2495		149.2462
47	$2s^22p^4$ ($^3_2$P) 3d ^{2}P	3	149.5805	–0.2430	0.0020	149.3398		149.3330
48	$2s^22p^4$ ($^3_2$P) 3p ^{4}D^o	1	149.7922	–0.2560	0.0073	149.5433		149.5757
49	$2s^22p^4$ ($^1_2$D) 3d ^{2}G	7	149.8926	–0.2900	0.0022	149.6049		149.5920
50	$2s^22p^4$ ($^1_2$D) 3d ^{2}G	9	150.1103	–0.3010	0.0022	149.8119		149.7946
51	$2s^22p^4$ ($^1_2$D) 3d ^{2}S	1	150.2959	–0.2690	0.0016	150.0282	150.323[b]	150.0119
52	$2s^22p^4$ (^{1}S) 3p ^{2}P	3	150.3095	–0.2810	0.0091	150.0377		150.0414
53	$2s^22p^4$ ($^1_2$D) 3d ^{2}D	5	150.3421	–0.2780	0.0018	150.0657	150.496[b]	150.0472
54	$2s^22p^4$ ($^1_2$D) 3d ^{2}P	3	150.5251	–0.2640	0.0014	150.2627	150.396[b]	150.2536
55	$2s^22p^4$ ($^1_2$D) 3d ^{2}F	7	150.5871	–0.2830	0.0020	150.3060		150.2872
56	$2s^22p^4$ ($^1_2$D) 3d ^{2}F	5	150.6393	–0.2770	0.0014	150.3632		150.3535
57	$2s^22p^4$ ($^1_2$D) 3d ^{2}D	3	151.3405	–0.2820	0.0019	151.0601	150.769[b]	151.0513
58	$2s2p^5$ ($^2_1$P) 3s ^{4}P^o	5	151.3955	–0.1360	–0.0765	151.1829		151.2128
59	$2s^22p^4$ ($^1_2$D) 3d ^{2}P	1	151.5784	–0.2940	0.0020	151.2863		151.2776
60	$2s2p^5$ ($^2_1$P) 3s ^{2}P^o	3	152.0811	–0.1280	–0.0766	151.8760		151.9190
61	$2s2p^5$ ($^2_1$P) 3s ^{4}P^o	3	153.6378	–0.1360	–0.0753	153.4264		153.4610
62	$2s2p^5$ ($^2_1$P) 3s ^{2}P^o	1	153.6572	–0.1340	–0.0752	153.4477		153.4761
63	$2s2p^5$ ($^2_1$P) 3p ^{4}S	3	155.0782	–0.0954	–0.1010	154.8812		154.9099
64	$2s^22p^4$ (^{1}S) 3d ^{2}D	5	155.3062	–0.3060	0.0048	155.0049		154.9880
65	$2s2p^5$ ($^2_1$P) 3p ^{2}D	5	155.3460	–0.1140	–0.0980	155.1344		155.1692
66	$2s^22p^4$ ($^3_2$P) 3d ^{2}D	3	155.5715	–0.3130	0.0072	155.2660		155.2641
67	$2s2p^5$ ($^2_1$P) 3p ^{4}D	7	156.2987	–0.1380	–0.0996	156.0610		156.0886
68	$2s2p^5$ ($^2_1$P) 3s ^{4}P^o	1	156.4514	–0.1960	–0.0686	156.1865		156.2207
69	$2s2p^5$ ($^2_1$P) 3p ^{2}P	3	156.4846	–0.1270	–0.0996	156.2585		156.2921
70	$2s2p^5$ ($^2_1$P) 3p ^{4}P	5	156.7161	–0.1270	–0.0996	156.4897		156.5317
71	$2s2p^5$ ($^2_1$P) 3p ^{4}P	1	157.0935	–0.1060	–0.0999	156.8880		156.9169
72	$2s2p^5$ ($^2_1$P) 3p ^{4}D	3	157.2615	–0.1200	–0.0994	157.0423		157.0727
73	$2s2p^5$ ($^2_1$P) 3p ^{2}S	1	157.3272	–0.1200	–0.1010	157.1062		157.1244
74	$2s2p^5$ ($^2_1$P) 3p ^{4}D	5	158.3708	–0.1420	–0.0980	158.1309		158.1542
75	$2s2p^5$ ($^2_1$P) 3p ^{2}D	3	158.4491	–0.1320	–0.0982	158.2186		158.2486
76	$2s2p^5$ ($^2_1$P) 3s ^{2}P^o	3	158.6248	–0.2070	–0.0705	158.3478		158.3534
77	$2s2p^5$ ($^2_1$P) 3s ^{2}P^o	1	158.9830	–0.2000	–0.0705	158.7128		158.7328
78	$2s2p^5$ ($^2_1$P) 3p ^{4}D	1	159.0928	–0.1320	–0.0971	158.8638		158.8938
79	$2s2p^5$ ($^2_1$P) 3p ^{2}P	1	160.3600	–0.1690	–0.0943	160.0963		160.1236
80	$2s2p^5$ ($^2_1$P) 3d ^{4}P^o	1	160.5228	–0.1130	–0.1010	160.3081		160.3148
81	$2s2p^5$ ($^2_1$P) 3d ^{4}P^o	3	160.7416	–0.1310	–0.1010	160.5089		160.5160
82	$2s2p^5$ ($^2_1$P) 3d ^{4}F^o	9	160.9886	–0.1700	–0.1020	160.7167		160.7266
83	$2s2p^5$ ($^2_1$P) 3d ^{4}D^o	5	161.0308	–0.1400	–0.1010	160.7898		160.7965
84	$2s2p^5$ ($^2_1$P) 3d ^{4}F^o	7	161.0495	–0.1580	–0.1010	160.7905		160.7975
85	$2s2p^5$ ($^2_1$P) 3p ^{4}P	3	161.2722	–0.1960	–0.0914	160.9851		161.0179
86	$2s2p^5$ ($^2_1$P) 3d ^{4}P^o	5	161.5790	–0.1480	–0.1010	161.3295		161.3372
87	$2s2p^5$ ($^2_1$P) 3d ^{2}F^o	7	161.6814	–0.1570	–0.1020	161.4230		161.4324
88	$2s2p^5$ ($^2_1$P) 3d ^{2}D^o	3	161.9737	–0.1400	–0.1010	161.7327		161.7398
89	$2s2p^5$ ($^2_1$P) 3p ^{2}D	3	162.3329	–0.1850	–0.0947	162.0531		162.0552
90	$2s2p^5$ ($^2_1$P) 3d ^{4}D^o	1	162.6953	–0.1500	–0.1010	162.4441		162.4565
91	$2s2p^5$ ($^2_1$P) 3d ^{2}P^o	1	163.0594	–0.1250	–0.1010	162.8336		162.8282
92	$2s2p^5$ ($^2_1$P) 3d ^{2}D^o	5	163.0882	–0.1540	–0.1000	162.8337		162.8285
93	$2s2p^5$ ($^2_1$P) 3d ^{4}D^o	3	163.1580	–0.1450	–0.1000	162.9132		162.9113
94	$2s2p^5$ ($^2_1$P) 3p ^{2}P	1	163.3121	–0.1670	–0.1000	163.0447		163.0404
95	$2s2p^5$ ($^2_1$P) 3d ^{4}D^o	7	163.3131	–0.1830	–0.0938	163.0362		163.0461

Table 2. (*Continued*).

S. No.	Configuration	2J	MCDF				Other results	FAC
			DC	Breit	QED	Total		
96	$2s2p^5$ ($^2_1$P) 3d ^{2}F^o	5	163.3326	–0.1580	–0.0998	163.0745		163.0747
97	$2s2p^5$ ($^2_1$P) 3p ^{2}D	5	163.5351	–0.2070	–0.0928	163.2348		163.2357
98	$2s2p^5$ ($^2_1$P) 3p ^{2}P	3	163.7246	–0.1970	–0.0930	163.4344		163.4374
99	$2s2p^5$ ($^2_1$P) 3p ^{2}S	1	163.7404	–0.1640	–0.0948	163.4812		163.4973
100	$2s2p^5$ ($^2_1$P) 3d ^{2}P^o	3	163.9610	–0.1650	–0.0994	163.6967		163.6996
101	$2s2p^5$ ($^2_1$P) 3d ^{4}F^o	5	166.1578	–0.2200	–0.0931	165.8451		165.8470
102	$2s2p^5$ ($^2_1$P) 3d ^{4}F^o	3	166.2214	–0.2110	–0.0938	165.9170		165.9255
103	$2s2p^5$ ($^2_1$P) 3d ^{2}F^o	5	168.1745	–0.2210	–0.0944	167.8593		167.8303
104	$2s2p^5$ ($^2_1$P) 3d ^{2}F^o	7	168.3433	–0.2330	–0.0944	168.0161		167.9798
105	$2s2p^5$ ($^2_1$P) 3d ^{2}P^o	3	168.4663	–0.2220	–0.0956	168.1483		168.1239
106	$2s2p^5$ ($^2_1$P) 3d ^{2}P^o	1	168.7325	–0.2320	–0.0955	168.4052		168.3919
107	$2s2p^5$ ($^2_1$P) 3d ^{2}D^o	5	168.7468	–0.2240	–0.0945	168.4286		168.3992
108	$2s2p^5$ ($^2_1$P) 3d ^{2}D^o	3	168.7766	–0.2210	–0.0941	168.4610		168.4426
109	$2p^6$ 3s ^{2}S	1	172.6953	–0.0813	–0.1680	172.4456		172.4763
110	$2p^6$ 3p ^{2}P^o	1	176.2001	–0.0561	–0.1930	175.9514		175.9813
111	$2p^6$ 3p ^{2}P^o	3	177.3918	–0.0815	–0.1910	177.1192		177.1476
112	$2p^6$ 3d ^{2}D	3	181.8909	–0.0917	–0.1940	181.6056		181.6010
113	$2p^6$ 3d ^{2}D	5	182.1606	–0.1050	–0.1940	181.8622		181.8567

[a]Ref. [28]. [b]Refs. [34] and [35].

A good agreement between the present calculations and the published data has been found. Taking NIST as a standard reference for comparison, we find that the maximum deviation between the present calculations and NIST energies and present results and Jönsson *et al.*[28] results is 0.84% for the level $2s2p^6\ ^2S_{1/2}$. The maximum disagreement of FAC calculations with our MCDF results is within 0.10%.

3.2. Radiative rates

For a transition $i \rightarrow j$, the relation between the absorption oscillator strength f_{ij} (dimensionless), and radiative rate A_{ji} (in s^{-1}) is expressed as

$$f_{ij} = \frac{mc}{8\pi^2 e^2}\lambda_{ji}^2 \frac{w_j}{w_i} A_{ji} = 1.49 \times 10^{-16} \lambda_{ji}^2 (w_j/w_i) A_{ji}. \quad (9)$$

In the above formula, m and e are the electron mass and charge respectively, c is the velocity of light, λ_{ji} denotes the transition wavelength in Å, and w_i and w_j are the statistical weights of the lower i and upper levels j respectively. Line strength may be defined as

$$S = S(i,j) = S(j,i) = \left|R_{ij}\right|^2,$$

where

$$R_{ij} = \left|\left\langle \psi_j \left| P \right| \psi_i \right\rangle\right|.$$

Here, ψ_i and ψ_j are the initial and final state wavefunctions, and R_{ij} represents the transition matrix element of the appropriate multipole operator P. The oscillator strength f_{ij} and line strength S_{ij} (in atomic units, a.u.) follow the following relations.

(i) For electric dipole transitions (E1),

$$A_{ji} = \frac{2.0261 \times 10^{18}}{w_j \lambda_{ji}^3} S_{ij}, \quad f_{ij} = \frac{303.75}{\lambda_{ji} w_i} S_{ij}. \quad (10)$$

(ii) For the magnetic dipole transitions (M1),

$$A_{ji} = \frac{2.6974 \times 10^{13}}{w_j \lambda_{ji}^3} S_{ij}, \quad f_{ij} = \frac{4.044 \times 10^{-3}}{\lambda_{ji} w_i} S_{ij}. \quad (11)$$

(iii) For electric quadrupole transitions (E2),

$$A_{ji} = \frac{1.1199 \times 10^{18}}{w_j \lambda_{ji}^5} S_{ij}, \quad f_{ij} = \frac{167.89}{\lambda_{ji}^3 w_i} S_{ij}. \quad (12)$$

(iv) For the magnetic quadrupole transitions (M2),

$$A_{ji} = \frac{1.4910 \times 10^{13}}{w_j \lambda_{ji}^5} S_{ij}, \quad f_{ij} = \frac{2.236 \times 10^{-3}}{\lambda_{ji}^3 w_i} S_{ij}. \quad (13)$$

In Table 3, we present the wavelengths (λ in Å), radiative rates (A_{ji} in s^{-1}), oscillator strengths (f_{ij} dimensionless), and line strengths (S_{ij} in a.u.) for some transitions determined from the ground level in length form only as it is considered to be more stable to the choice of configurations and hence more accurate. There are 50 electric dipole, 53 electric quadrupole, 47 magnetic dipole, and 56 magnetic quadrupole transitions among 113 levels from the ground level. Some out of these are presented in Table 3.

As the ratio of velocity/length is an indicator of accuracy of f- or A-values, we have also provided the ratios between length and velocity forms. A good agreement between the two forms is always desirable, but not a necessary condition for accuracy. The vel./len ratio in our case is generally within 10% of unity for most of the strong transitions ($f \geq 0.1$). For some strong transitions such as $2s^22p^5\ ^2P^o_{3/2}$–$2s^22p^4\ (^1_0S)\ 3s\ ^2S_{1/2}$ the ratio is exactly unity. For weaker transitions ($f \sim 10^{-5}$ or less), such as $2s^22p^5\ ^2P^o_{3/2}$–$2s^22p^4\ (^3_2P)\ 3d\ ^4D_{5/2}$, the ratio is sometimes higher.

Table 3. Transition data for E1, E2, M1, M2 transitions for Rb XXIX from $2s^2 2p^5\ ^2P^o_{3/2}$: lower level i, upper level j, wavelength λ (in Å), transition rate A_{ji} (s^{-1}) (length form), oscillator strength f_{ij} (length form), line strength S_{ij} (in a.u.) (length form).

Levels		MCDF					Type of transition
i	j	λ/Å	A_{ji}/s^{-1}	f_{ij}	S_{ij}/ a.u.	Vel/len	
1	3	4.932×10^{1}	2.52×10^{11}	4.60×10^{-2}	2.99×10^{-2}	0.93	E1
1	4	6.767×10^{0}	1.10×10^{12}	1.13×10^{-2}	1.01×10^{-3}	0.97	E1
1	5	6.749×10^{0}	9.84×10^{12}	6.72×10^{-2}	5.97×10^{-3}	0.98	E1
1	6	6.685×10^{0}	4.25×10^{12}	1.42×10^{-2}	1.25×10^{-3}	1.00	E1
1	9	6.553×10^{0}	2.48×10^{12}	1.60×10^{-2}	1.38×10^{-3}	0.98	E1
1	10	6.539×10^{0}	3.91×10^{12}	1.25×10^{-2}	1.08×10^{-3}	0.98	E1
1	15	6.506×10^{0}	5.10×10^{12}	4.85×10^{-2}	4.16×10^{-3}	0.97	E1
1	16	6.500×10^{0}	8.78×10^{11}	5.56×10^{-3}	4.76×10^{-4}	0.98	E1
1	23	6.320×10^{0}	4.94×10^{10}	2.96×10^{-4}	2.46×10^{-5}	0.93	E1
1	24	6.320×10^{0}	2.68×10^{7}	2.41×10^{-7}	2.01×10^{-8}	4.50	E1
1	27	6.314×10^{0}	1.31×10^{12}	3.91×10^{-3}	3.25×10^{-4}	0.94	E1
1	2	1.987×10^{2}	1.05×10^{3}	3.12×10^{-9}	5.82×10^{-4}	1.00	E2
1	7	6.585×10^{0}	4.55×10^{9}	2.96×10^{-5}	2.01×10^{-4}	0.98	E2
1	8	6.578×10^{0}	1.25×10^{10}	1.21×10^{-4}	8.23×10^{-4}	0.98	E2
1	11	6.534×10^{0}	1.31×10^{10}	4.18×10^{-5}	2.78×10^{-4}	0.97	E2
1	12	6.528×10^{0}	9.56×10^{9}	9.16×10^{-5}	6.07×10^{-4}	0.98	E2
1	13	6.525×10^{0}	3.22×10^{9}	4.11×10^{-5}	2.72×10^{-4}	0.98	E2
1	14	6.500×10^{0}	2.84×10^{9}	9.00×10^{-6}	5.89×10^{-5}	1.00	E2
1	17	6.467×10^{0}	1.71×10^{10}	1.07×10^{-4}	6.91×10^{-4}	0.98	E2
1	18	6.443×10^{0}	1.10×10^{9}	6.85×10^{-6}	4.36×10^{-5}	1.00	E2
1	19	6.387×10^{0}	4.30×10^{8}	1.32×10^{-6}	8.17×10^{-6}	0.96	E2
1	20	6.370×10^{0}	3.61×10^{8}	2.20×10^{-6}	1.35×10^{-5}	0.94	E2
1	21	6.337×10^{0}	5.80×10^{7}	5.24×10^{-7}	3.18×10^{-6}	1.00	E2
1	22	6.331×10^{0}	3.92×10^{9}	3.53×10^{-5}	2.13×10^{-4}	0.98	E2
1	25	6.320×10^{0}	5.35×10^{9}	1.60×10^{-5}	9.63×10^{-5}	0.96	E2
1	26	6.318×10^{0}	8.28×10^{9}	4.95×10^{-5}	2.98×10^{-4}	0.98	E2
1	2	1.987×10^{2}	2.27×10^{6}	6.73×10^{-6}	1.32×10^{0}		M1
1	7	6.585×10^{0}	2.15×10^{7}	1.40×10^{-7}	9.13×10^{-4}		M1
1	8	6.578×10^{0}	4.07×10^{6}	3.96×10^{-8}	2.58×10^{-4}		M1
1	11	6.534×10^{0}	1.79×10^{7}	5.71×10^{-8}	3.69×10^{-4}		M1
1	12	6.528×10^{0}	1.62×10^{6}	1.55×10^{-8}	1.00×10^{-4}		M1
1	14	6.500×10^{0}	1.29×10^{6}	4.09×10^{-9}	2.63×10^{-5}		M1
1	17	6.467×10^{0}	1.28×10^{5}	7.99×10^{-10}	5.11×10^{-6}		M1
1	18	6.443×10^{0}	8.36×10^{5}	5.20×10^{-9}	3.32×10^{-5}		M1
1	19	6.387×10^{0}	2.38×10^{5}	7.28×10^{-10}	4.60×10^{-6}		M1
1	20	6.370×10^{0}	5.95×10^{5}	3.62×10^{-9}	2.28×10^{-5}		M1
1	21	6.337×10^{0}	9.45×10^{5}	8.53×10^{-9}	5.35×10^{-5}		M1
1	22	6.331×10^{0}	5.92×10^{6}	5.33×10^{-8}	3.34×10^{-4}		M1
1	25	6.320×10^{0}	4.30×10^{6}	1.29×10^{-8}	8.04×10^{-5}		M1
1	26	6.318×10^{0}	2.29×10^{6}	1.37×10^{-8}	8.56×10^{-5}		M1
1	3	4.932×10^{1}	1.29×10^{4}	2.36×10^{-9}	5.06×10^{-1}		M2
1	4	6.767×10^{0}	1.36×10^{7}	1.40×10^{-7}	7.78×10^{-2}		M2
1	5	6.749×10^{0}	2.77×10^{6}	1.89×10^{-8}	1.04×10^{-2}		M2
1	6	6.685×10^{0}	1.26×10^{7}	4.22×10^{-8}	2.26×10^{-2}		M2
1	9	6.553×10^{0}	3.12×10^{4}	2.01×10^{-10}	1.01×10^{-4}		M2
1	10	6.539×10^{0}	3.67×10^{5}	1.18×10^{-9}	5.89×10^{-4}		M2
1	15	6.506×10^{0}	3.83×10^{5}	3.65×10^{-9}	1.80×10^{-3}		M2
1	16	6.500×10^{0}	2.96×10^{5}	1.87×10^{-9}	9.21×10^{-4}		M2
1	23	6.320×10^{0}	8.65×10^{2}	5.18×10^{-12}	2.34×10^{-6}		M2
1	24	6.320×10^{0}	4.40×10^{5}	3.95×10^{-9}	1.79×10^{-3}		M2
1	27	6.314×10^{0}	8.57×10^{7}	2.56×10^{-7}	1.15×10^{-1}		M2
1	28	6.315×10^{0}	1.50×10^{8}	1.79×10^{-6}	8.06×10^{-1}		M2
1	30	6.302×10^{0}	1.06×10^{8}	1.26×10^{-6}	5.63×10^{-1}		M2

In Table 4, we have compared our calculated wavelengths of Rb XXIX with those compiled by NIST and other observed results by Denis–Petit *et al.*[33] We observe that our results agree well with both of them.

Table 4. Comparison of computed wavelengths (in Å) with observed wavelengths from NIST and other available results for transitions from $2s^22p^5\ ^2P^o_{3/2}$ to selected upper levels for Rb XXIX.

S. No.	Levels		2J		(λ/Å) MCDF	(λ/Å) NIST	Ref. [33]	Transition type
	Lower	Upper	i	j				
1	$2s^22p^5\ ^2P^o$	$2s^22p^4\ (^1_0S)\ 3d\ ^2D$	3	3	6.235	6.031		E1
2	$2s^22p^5\ ^2P^o$	$2s^22p^4\ (^1_2D)\ 3d\ ^2D$	3	3	6.032	6.044		E1
3	$2s^22p^5\ ^2P^o$	$2s^22p^4\ (^1_2D)\ 3d\ ^2D$	3	5	6.072	6.055		E1
4	$2s^22p^5\ ^2P^o$	$2s^22p^4\ (^1_2D)\ 3d\ ^2P$	3	3	6.065	6.059	6.054	E1
5	$2s^22p^5\ ^2P^o$	$2s^22p^4\ (^1_2D)\ 3d\ ^2S$	3	1	6.074	6.062		E1
6	$2s^22p^5\ ^2P^o$	$2s^22p^4\ (^3_2P)\ 3d\ ^2D$	3	5	6.112	6.107		E1
7	$2s^22p^5\ ^2P^o$	$2s^22p^4\ (^3_2P)\ 3d\ ^2D$	3	3	5.869	6.122		E1
8	$2s^22p^5\ ^2P^o$	$2s^22p^4\ (^3_2P)\ 3d\ ^4F$	3	5	6.223	6.231		E1
9	$2s^22p^5\ ^2P^o$	$2s^22p^4\ (^3_2P)\ 3d\ ^4P$	3	3	6.269	6.251		E1
10	$2s^22p^5\ ^2P^o$	$2s^22p^4\ (^3_2P)\ 3s\ ^2D$	3	5	6.506	6.502		E1
11	$2s^22p^5\ ^2P^o$	$2s^22p^4\ (^3_2P)\ 3s\ ^2P$	3	3	6.749	6.741	6.742	E1
12	$2s^22p^5\ ^2P^o$	$2s2p^6\ ^2S$	3	1	49.316	49.728		E1
13	$2s^22p^5\ ^2P^o$	$2s^22p^5\ ^2P^o$	3	1	198.660	198.270		M1
14	$2s^22p^5\ ^2P^o$	$2s2p^5\ (^2_1P)\ 3p\ ^2D$	3	3	5.623		5.622	E1
15	$2s^22p^5\ ^2P^o$	$2s2p^5\ (^2_1P)\ 3p\ ^4D$	3	5	5.763		5.737	E1
16	$2s^22p^5\ ^2P^o$	$2s2p^5\ (^2_1P)\ 3p\ ^2S$	3	1	5.800		5.799	E1
17	$2s^22p^5\ ^2P^o$	$2s2p^5\ (^2_1P)\ 3p\ ^4P$	3	5	5.823		5.819E	E1
18	$2s^22p^5\ ^2P^o$	$2s2p^5\ (^2_1P)\ 3p\ ^2P$	3	3	5.832		5.825	E1
19	$2s^22p^5\ ^2P^o$	$2s2p^5\ (^2_1P)\ 3p\ ^2D$	3	5	5.874		5.868	E1
20	$2s^22p^5\ ^2P^o$	$2s^22p^4\ (^1_2D)\ 3d\ ^2F$	3	5	6.061		6.067	E1
21	$2s^22p^5\ ^2P^o$	$2s^22p^4\ (^3_2P)\ 3d\ ^2F$	3	5	6.106		6.102	E1
22	$2s^22p^5\ ^2P^o$	$2s^22p^4\ (^3_2P)\ 3d\ ^4P$	3	5	6.256		6.247	E1

3.3. Study of EUV and soft x-ray transitions

In the present paper, we have presented our calculated wavelengths of EUV and soft x-ray transitions in Table 3 by exciting a single electron from the L-shell. We have identified an EUV and 108 soft x-ray (SXR) transitions among the lowest 113 levels from the ground level. The transition $2s^22p^5\ ^2P^o_{3/2}$–$2s^22p^5\ ^2P^o_{1/2}$ lies in the EUV region and all other transitions $2s^22p^5\ ^2P^o$–$2s^22p^43l$ ($l = s, p, d$) are SXR.

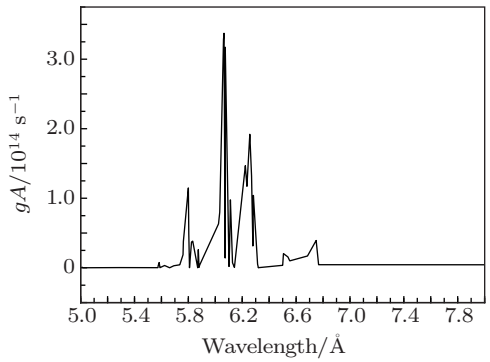


Fig. 1. gA spectra of Rb XXIX within SXR region for E1 transitions.

In Table 3, there is a sudden decrease in the wavelength of the SXR photon from 49.32 Å to 6.767 Å which may be due to the increase in force of repulsion between inner and valence electrons thereby increasing transition energy. We have plotted gA spectra of Rb XXIX with SXR region for E1 and M2 transitions in Figs. 1 and 2 respectively, where g denotes the statistical weight of lower level.

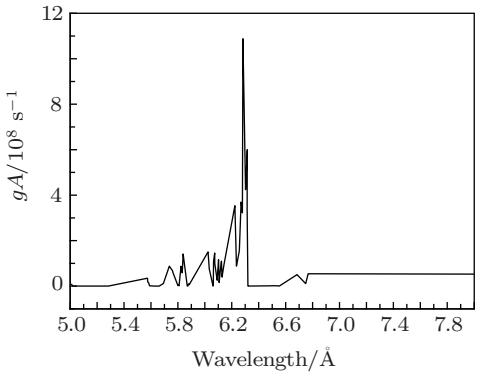


Fig. 2. gA spectra of Rb XXIX within SXR region for M2 transitions.

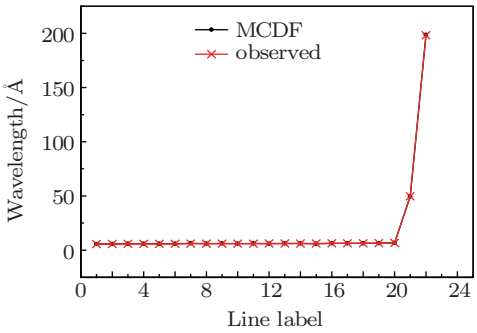


Fig. 3. (color online) Circle and cross markers represent MCDF and observed wavelengths respectively.

In Fig. 3, we have plotted a comparison between our calculated SXR wavelengths and observed wavelengths from other available results. The horizontal axis titled 'Line label' represents the labeling of transitions as represented in the first column of Table 4.

4. Lifetimes

The lifetime (τ) for a level j for a transition $i \rightarrow j$ is defined as follows:

$$\tau_j = \frac{1}{\sum_i A_{ji}}. \quad (14)$$

In Table 1, we have provided lifetimes for all 113 levels from our calculations. These include A-values from all types of transitions, i.e., E1, E2, M1, and M2. It provides a check on the accuracy of the calculations, as it is a measurable quantity. To our knowledge, there are no results available for lifetimes for Rb XXIX to compare. We hope that the present results will be beneficial for future comparisons. These may encourage experimentalists to measure lifetimes, particularly for levels $2s^2 2p^5\ {}^2P^o_{1/2}$, $2s^2 2p^4\ ({}^3_2P)\ 3p\ {}^4P^o_{1/2}$ which have comparatively a larger value of lifetime.

5. Conclusion

In this paper, we have reported energy levels for the lowest 113 levels and radiative rates for E1, E2, M1, and M2 transitions from the ground level of Rb XXIX. Two independent calculations have been carried out using the MCDF and FAC codes. A comparison between the two sets of energy levels, as well as with the other available results, shows a satisfactory agreement. Wavefunction composition has been provided in both *LSJ* and *JJ* couplings. Though every care has been taken to identify the levels based on the strength of their eigenvectors, a possibility of their re-designation still remains. EUV and SXR transition wavelengths have been calculated using MCDF method. Comparisons have also been provided, for transition wavelengths for some selected transitions with NIST and other observed values are found to be in good agreement. The vel/len ratio is within 10% of unity, in particular the strong transitions with $f \geq 0.1$ confirms the accuracy of our results.

Finally, the lifetimes for all 113 levels have been reported, although, due to paucity of data no comparisons with measured values are possible. However, our calculations will be helpful for an accuracy assessment for future measurement of lifetimes.

We have obtained new and previously unpublished energy levels, oscillator strengths, and transition probabilities for Rb XXIX. Hopefully, the present wide range of data will be useful in astrophysics, modeling of a variety of plasmas and for line identification in future experimental work.

Acknowledgments

Indu Khatri and Arun Goyal are thankful to U. G. C., India for their Junior Research Fellowship. M. M. is thankful to U. G. C. for Basic Science Research Fellowship.

References

[1] Aller L H 1984 *Physics of Thermal Gaseous Nebulae* (Dordrecht: Reidel)
[2] Dere K P 1978 *Astrophys. J.* **221** 1062
[3] Doyle J G 1983 *Solar Phys.* **89** 115
[4] Stratton B C, Moos H W, Suckewer S, Feldman U, Seely J F and Bhatia A K 1985 *Phys. Rev. A* **31** 2534
[5] Suckewer S, Fonk R and Hinnov E 1980 *Phys. Rev. A* **21** 924
[6] Edlén B 1969 *Sol. Phys.* **9** 439
[7] Drawin H W 1981 *Phys. Scr.* **24** 622
[8] Sudkewer S 1981 *Phys. Scr.* **23** 72
[9] Suckewer S and Hinnov E 1978 *Phys. Rev. Lett.* **41** 756
[10] Doschek G A and Feldman U 1976 *J. Appl. Phys.* **47** 3083
[11] Edlén B 1984 *Phys. Scripta* **T8** 5
[12] Träbert E, Heckmann P H, Hutton R and Martinson I 1988 *J. Opt. Soc. Am B* **5** 2173
[13] Ellis D G, Martinson I and Träbert E 1989 *Comm. At. Mol. Phys.* **22** 241
[14] Seaton M J 1987 *J. Phys. B* **20** 6363
[15] Lambert D L and Warner B 1968 *Mon. Not. R. Astron. Soc.* **140** 197
[16] Sampson D H, Zhang H L and Fontes C J 1991 *At. Data Nucl. Data Tables* **48** 25
[17] Ivanova E P and Gulov A V 1991 *At. Data Nucl. Data Tables* **49** 1
[18] Kim Y K and Huang K N 1982 *Phys. Rev. A* **26** 1984
[19] Rodrigues G C, Indelicato P, Santos J P, Patté P and Parente F 2004 *At. Data Nucl. Data Tables* **86** 117
[20] Gu M F 2005 *At. Data Nucl. Data Tables* **89** 267
[21] Cheng K T, Kim Y K and Desclaux J P 1979 *At. Data Nucl. Data Tables* **24** 111
[22] Edlén B 1983 *Phys. Scr.* **28** 51
[23] Mohan M and Hibbert A 1991 *Phys. Scr.* **44** 158
[24] Blackford H M S and Hibbert A 1994 *At. Data Nucl. Data Tables* **58** 101
[25] Nahar S N 2006 *Astronom. Astrophys.* **457** 721
[26] Fischer C F and Tachiev G 2004 *At. Data Nucl. Data Tables* **87** 1
[27] Jonauskas V, Keenan F P, Foord M E, Heeter R F, Rose S J, van Hoof P A M, Ferland G J, Aggarwal K M, Kisielius R and Norrington P H 2004 *Astronom. Astrophys.* **416** 383
[28] Jönsson P, Alkauskas A and Gaigalas G 2013 *At. Data Nucl. Data Tables* **99** 431
[29] Feldman U, Ekberg J O, Seely J F, Brown C M, Kania D R, MacGowan B J and Keane C J 1991 *J. Opt. Soc. Am. B* **8** 531
[30] Feldman U, Seely J F, Behring W E, Richardson M C and Goldsmith S 1985 *J. Opt. Soc. Am. B* **2** 1658
[31] Zigler A, Feldman U and Doschek G A 1986 *J. Opt. Soc. Am. B* **3** 1221
[32] Hutcheon R J, Cooke L, Key M H, Lewis C L S and Bromage G E 1980 *Phys. Scr.* **21** 89
[33] Denis P D, Comet M, Bonnet T, Hannachi F, Gobet F, Tarisien M, Versteegen M, Gosselin G, Méot V, Morel P, Pain J-Ch, Gilleron F, Frank A, Bagnoud V, Blazevic A, Dorchies F, Peyrusse O, Cayzac W and Roth M 2014 *J. Quant. Spectrosc. Radiat. Transf.* **148** 70
[34] Kramida A, Ralchenko Y and Reader J 2015 *NIST ASD Team, NIST Atomic Spectra Database* (Ver. 5.3), [Online]. Available: http://physics.nist.gov/asd [2016, January 15] (National Institute of Standards and Technology, Gaithersburg, MD)
[35] Sansonetti J E 2006 *J. Phys. Chem. Ref. Data* **35** 301
[36] Goyal A, Khatri I, Aggarwal S, Singh A K and Mohan M 2015 *J. Quant. Spectrosc. Radiat. Transf.* **161** 157
[37] Grant I P, Mckenzie B J, Norrington P H, Mayers D F and Pyper N C 1980 *Comput. Phys. Commun.* **21** 207
[38] Norrington P H 2009 http://www.am.qub.ac.uk/DARC/
[39] Quinet P 2012 *J. Phys. B* **45** 025003
[40] Singh A K, Aggarwal S and Mohan M 2013 *Phys. Scr.* **88** 035301
[41] Khatri I, Goyal A, Aggarwal S, Singh A K and Mohan M 2015 *Chin. Phys. B* **24** 103202
[42] Aggarwal K M, Keenan F P and Msezane A Z 2003 *At. Data Nucl. Data Tables* **85** 453
[43] Goyal A, Khatri I, Aggarwal S, Singh A K and Mohan M 2013 *Can. J. Phys.* **91** 394
[44] Aggarwal S, Jha A K S, Khatri I, Singh N and Mohan M 2015 *Chin. Phys. B* **24** 103202
[45] Gu M F 2008 *Can. J. Phys.* **86** 675